Title

Field evaluation of the versatile aerosol concentration enrichment system (VACES) particle concentrator coupled to the rapid single-particle mass spectrometer (RSMS-3)

Journal

Journal of Geophysical Research-Atmospheres, 110(D7)

ISSN

0148-0227

Authors

Zhao, Yongjing
Bein, K J
Wexler, A S
et al.

Publication Date

2005-02-01

DOI

10.1029/2004JD004644

Peer reviewed

Field evaluation of the versatile aerosol concentration enrichment system (VACES) particle concentrator coupled to the rapid single-particle mass spectrometer (RSMS-3)

Y. Zhao,[1] K. J. Bein,[2] A. S. Wexler,[1,2,3] C. Misra,[4] P. M. Fine,[4] and C. Sioutas[4]

Received 13 February 2004; revised 28 July 2004; accepted 3 August 2004; published XX Month 2005.

[1] A field evaluation of versatile aerosol concentration enrichment system (VACES) coupled to a rapid single-particle mass spectrometer (RSMS-3) was conducted as part of the U.S. Environmental Protection Agency Supersite program in Pittsburgh during March 2002. RSMS-3 hit rate increases were measured, and possible particle composition changes introduced by the VACES were examined in the single-particle mass spectra. The hit rates increased by 5–20 times at particle sizes ranging from 40 to 640 nm. VACES only enhances the hit rate by about a factor of 2 for large particle sizes because the RSMS-3 flow rates for these particles did not match the optimum operating condition of VACES. During the 3 days of measurements most of the particles were a mixture of carbonaceous material and ammonium nitrate with a variation across the spectrum from particles that were mostly carbonaceous to particles that were mostly ammonium nitrate. Both ambient and concentrated carbonaceous and ammonium nitrate composition distributions were indistinguishable with RSMS-3, suggesting that VACES introduces an insignificant artifact for those particles.

Citation: Zhao, Y., K. J. Bein, A. S. Wexler, C. Misra, P. M. Fine, and C. Sioutas (2005), Field evaluation of the versatile aerosol concentration enrichment system (VACES) particle concentrator coupled to the rapid single-particle mass spectrometer (RSMS-3), *J. Geophys. Res.*, *110*, D07S02, doi:10.1029/2004JD004644.

1. Introduction

[2] Atmospheric ultrafine particles are either formed by gas-to-particle conversion processes, in which hot and supersaturated vapors undergo condensation upon being cooled to ambient temperatures, or directly emitted as products of incomplete combustion processes [*Finlayson-Pitts and Pitts*, 1986]. Although the mass fraction of the ultrafine mode is negligible, this size range contains the highest number of ambient particles as well as the highest total surface area. Because of their increased number and surface area, ultrafine particles are particularly important in atmospheric chemistry and environmental health.

[3] Recently, increasing toxicological and epidemiological evidence supports the link between respiratory health effects and exposures to ultrafine particles. Recent epidemiological studies [*Heyder et al.*, 1996; *Peters et al.*, 1997] demonstrate a stronger association between health effects and exposures to ultrafine particles compared to accumulation mode or coarse particles. Toxicological studies by *Donaldson et al.* [1998] indicate that ultrafine particles exerted a stronger physiological effect than the same mass of coarse or fine particles. A recent study by *Li et al.* [2003] indicates that ultrafine particulate matter (PM) is most potent in inducing cellular heme oxygenase-1 (HO-1) expression and depleting intracellular glutathione, both sensitive markers for oxidative stress, compared to concurrently collected accumulation and coarse mode PM. The same study showed that ultrafine particles, and to a lesser extent fine particles, localize in mitochondria where they induce major structural damage.

[4] A rapid single-particle mass spectrometer (RSMS) was developed at the University of California, Davis, and the University of Delaware [*Phares et al.*, 2002] for measuring the size and chemical composition of individual atmospheric fine and ultrafine single particles. The second generation of the single-particle mass spectrometer, RSMS-2, was deployed at the U.S. Environmental Protection Agency (EPA) Supersite in Atlanta in August 1999 [*Rhoads et al.*, 2003] and in Houston from 23 August to 18 September 2000 [*Phares et al.*, 2003]. Over 15,000 individual particles were recorded covering 14–1300 nm size range and composing of 70 compound classes in the Atlanta Supersite experiment. In Houston, transient plumes of ultrafine particles that were present at the site for short duration were detected because of the instrument's fine temporal resolution and its ability to run continuously for a period of time. The RSMS-2 was modified to its third generation, RSMS-3, in 2001. In comparison with RSMS-2, there are two major improvements in RSMS-3: (1) both

[1]Department of Mechanical and Aeronautical Engineering, University of California, Davis, California, USA.
[2]Department of Land, Air, and Water Resources, University of California, Davis, California, USA.
[3]Department of Civil and Environmental Engineering, University of California, Davis, California, USA.
[4]Department of Civil and Environmental Engineering, University of Southern California, Los Angeles, California, USA.

0148-0227/05/2004JD004644$09.00

positive and negative ions can be detected and (2) two of the four digitizer channels are used to record each ion polarity signal to increase the spectral dynamic range (one channel is set at low sensitivity for strong signals and the other at high sensitivity for weak signals) and then signals in the two channels are combined by a computer program. One RSMS-3 was installed at the U.S. EPA Supersite in Pittsburgh. A quarter of million single-particle mass spectra were analyzed over a 1 year period from September 2001 to October 2002. Results indicate that a rich array of multicomponent ultrafine particles were present [*Bein et al.*, 2005]. Another RSMS-3 was installed at the U.S. EPA Supersite in Baltimore for semicontinuous operation over 9 months from 2001 to 2002 [*Lake et al.*, 2003; *Tolocka et al.*, 2005], where the characteristics of specific chemical components, such as metals [*Tolocka et al.*, 2004a], sulfate [*Lake et al.*, 2004], and nitrate [*Tolocka et al.*, 2004b], and association among multiple components in the same particle were examined. A disadvantage of the RSMS-3 single-particle instrument is its insufficient hit rate for all but polluted urban conditions. Laboratory tests showed that the detection efficiency of RSMS was about one in a million and varied with particle size, shape, and composition [*Kane and Johnston*, 2000; *Phares et al.*, 2002]. In order to increase the RSMS hit rate for cleaner conditions and therefore to broaden its applicability, several methods are under consideration. The goal is to either increase the sampling efficiency without changing its sizing ability or concentrate particles before they enter the instrument. Theoretical work shows that the hit rate may be increased by more than 10 times using a new inlet system with capped cone structure [*Middha and Wexler*, 2003]. Another way to increase the hit rate is to introduce a particle concentrator to the sampling inlet of the RSMS-3 mass spectrometer, which is the topic of this presentation.

[5] A particle concentrator (versatile aerosol concentration enrichment system, VACES) has been developed at the University of Southern California and deployed in many field experiments [*Sioutas et al.*, 1999; *Kim et al.*, 2001a, 2001b]. In its optimum configuration, VACES concentrates fine particles, including the ultrafine mode, by a factor up to 30, depending on the ratio of total-to-minor flow rates of the virtual impactor [*Sioutas et al.*, 1999; *Kim et al.*, 2001a, 2001b]. Evaluation of the VACES was previously performed in both laboratory and field and the results are described in a great detail by *Kim et al.* [2000, 2001a, 2001b] and *Geller et al.* [2002]. The ability of the VACES to concentrate particles has been laboratory tested using different type of particles, including polystyrene latex (PSL), silica beads, ammonia sulfate, and ammonia nitrate, in the size range from 50 to 1900 nm and at three minor flow rates of 7, 10, and 20 liters per minute (lpm) with the major intake flow rate of 220 lpm. TSI Condensation Particle Counter (CPC) was used to measure the number concentration of the original aerosols at upstream and concentrated aerosols at the downstream of the VACES. TSI Scanning Mobil Particle Sizer (SMPS) was used to measure the size distribution of those aerosols. The resulting enrichment factors (ratio of downstream aerosol number concentration to upstream) were very close to the ideal values (ratio of total-to-minor flow rate) and the aerosol size distribution was fairly well preserved during the concentration enrichment process. Hygroscopic aerosols, such as ammonium sulfate and ammonia nitrate were concentrated as efficiently as hydrophobic PSL particles [*Kim et al.*, 2001a]. Field evaluations of the VACES were conducted outdoors in Southern California [*Geller et al.*, 2002; *Kim et al.*, 2001b], where measurements of concentration-enriched aerosols were compared to direct ambient measurements made with micro-orifice uniform deposit impactor (MOUDI). Downstream and upstream measurements showed very good agreement (correlation coefficient r^2 = 0.80 for coarse particles, 0.66 for $PM_{2.5}$ nitrate, 0.84 for $PM_{2.5}$ sulfate, and 0.94 for ultrafine elemental carbon). Averaged concentration enrichment of those aerosols was very close to the ideal values. These experimental results indicated that the concentrator does not distort the size distribution of the original ultrafine aerosols on the basis of bulk measurements of particle chemical composition. Comparisons between the VACES and a reference monitor for ammonium nitrate, the Harvard/EPA Annular Denuder System, HEADS [*Koutrakis et al.*, 1988], shows excellent agreement between the nitrate concentrations between HEADS and VACES [*Kim et al.*, 2000].

[6] A field evaluation of the VACES concentrator coupled to the RSMS-3 ultrafine single-particle mass spectrometer was conducted at the Pittsburgh EPA Supersite in March 2002 to determine the hit rate increase and elucidate possible particle composition changes introduced by the concentrator, on the basis of single-particle mass spectra.

2. Methods

2.1. Instrumental Setup

[7] Figure 1 shows a schematic diagram of rapid single-particle mass spectrometer, RSMS-3. The principle of RSMS-3 is nearly the same as RSMS-2, which has been described in detail previously [*Phares et al.*, 2002], so only a brief description is given here. RSMS-3 consists of a Nafion dryer (PD-750-12SS, Perma Pure Inc., Toms River, New Jersey), a rotary valve orifice bank, an inlet system, two liners jointed with a source region, two Microchannel Plate (MCP) detectors (25 mm BiPolar Time-of-Flight, Burle Opto-Electronics Inc., Sturbridge, Massachusetts), and an UV ArF Excimer laser (EX10, GAM Laser Inc., Orlando, Florida). Sample air with particles passes through a dryer and a rotary valve orifice bank and then arrives at the inlet system composed of an aerodynamic lens with four vacuum stages. A 3 lpm carrying dry air passes through the dryer and removes primarily water vapor from the sample. The orifice bank controls inlet pressure. The inlet system creates a particle beam with a narrow particle size range and skims off most of the gas. The optimum particle size that is focused depends on the upstream pressure, which is controlled by the rotary valve orifice bank. A 193 nm, pulsed UV laser beam from an ArF Excimer laser is aligned coaxially with the particle beam by a 45° folding-aligning mirror and focused at the source region by a lens. The laser emits laser pulses at 50 or 100 Hz and the laser energy is between 5 and 8 mJ. When the laser beam hits a particle in the source region, the particle is ablated and ionized. Positive ions are accelerated by an electric field and fly inside the liner to the MCP detector on the positive side of the instrument. Negative ions fly in the opposite direction

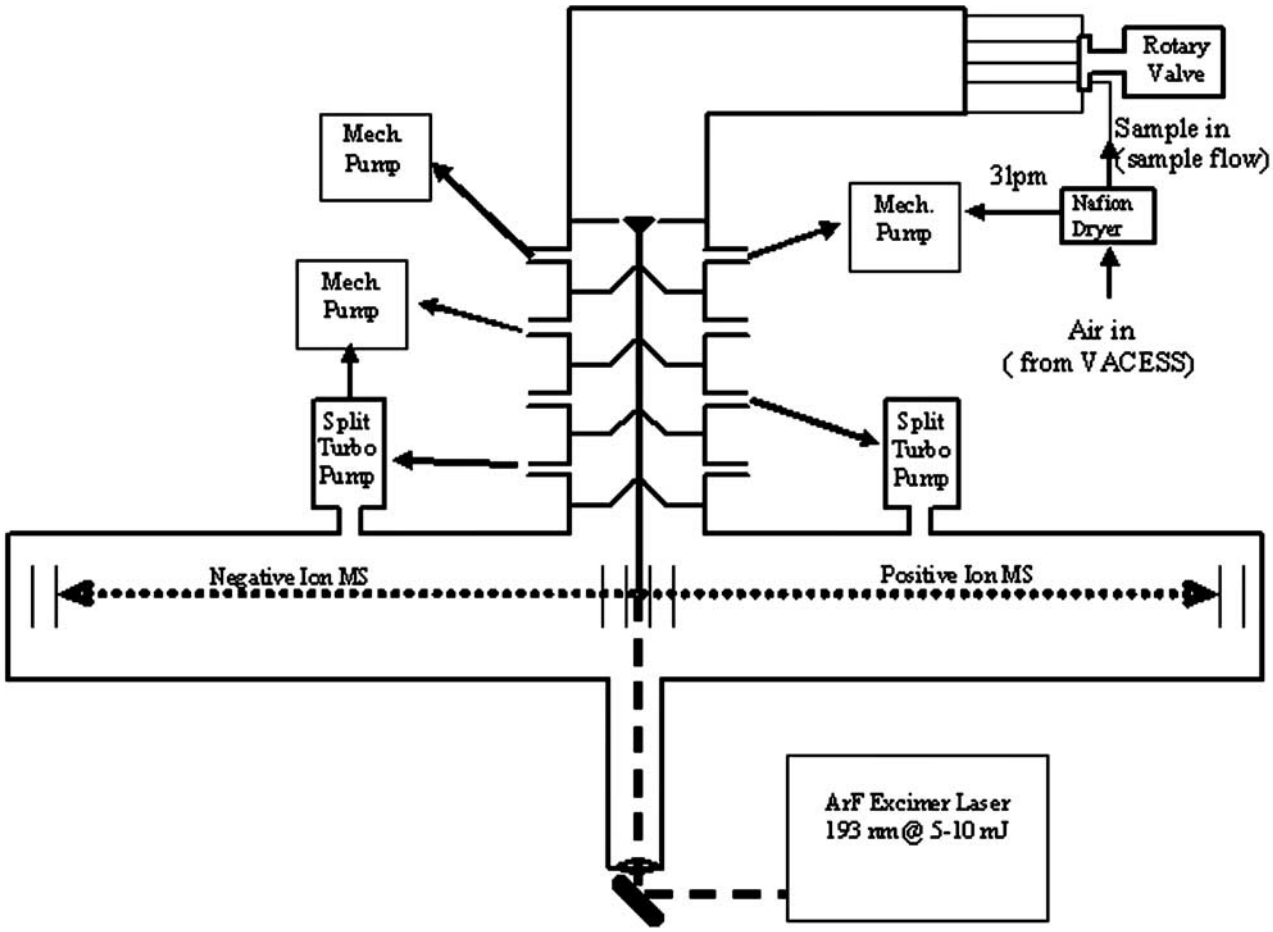

Figure 1. Schematic diagram of rapid single-particle mass spectrometer (RSMS-3).

and are detected by another MCP on the negative side. Signals from the MCP detectors are digitized by a four-channel A/D converter (two A/D channels for each MCP signal to increase dynamic range) and recorded by a computer. There are nine orifices in the orifice bank, so RSMS-3 can measure nine particle sizes. Table 1 lists the inlet pressure, flow rates, and particle sizes (Stokes number = 1.14) at each orifice. The 3 lpm air drawn from the Nafion dryer was not included in Table 1, but shown in Figure 1.

[8] Figure 2 is a schematic diagram of VACES fine plus ultrafine particle concentrator. The VACES consists of a sample line, a saturation-condensation system, a virtual impactor, and a diffusion dryer (Model 3062, TSI Inc. Shoreview, Minnesota). Sample air is drawn through the sample line into a 35°C saturation chamber above a warm DI water bath where particles and air are humidified. This warm saturated aerosol is then introduced into a section cooled by 10°C, thereby supersaturating the air and causing rapid condensation and particle growth. A virtual impactor concentrates the particles in its minor flow, which is then dehydrated so the particles return to their original sizes by means of a series of diffusion dryers. Particle enrichment by the VACES concentrator depends on the ratio of the virtual impactor's total-to-minor flow rates [*Sioutas et al.*, 1999; *Kim et al.*, 2001a]. The principle of a virtual impactor is similar to that of an inertial impactor [e.g., *Willeke and Baron*, 1993]: both methods use particulate inertia to separate particles from gases. A jet of particle-laden air is injected at a collection medium, which causes an abrupt deflection of the air streamlines. Particles larger than a certain size (the so-called cut point of the impactor) cross the air streamlines and, in the case of an inertial impactor, are collected on the medium, while particles smaller than a certain size follow the deflected streamlines. The main difference between an inertial and a virtual impactor is that in the latter, particles are injected into a collection probe rather than onto a collection medium. To separate larger particles continuously from the collection

Table 1. RSMS-3 Sizing Ability and Sample Flow Rates

Orifice	Orifice ID, inches/mm	Inlet Pressure, torr	Sample Flow Rate,[a] lpm	Sizing, nm
1	0.063/1.600	151.7	15.4	1100
2	0.035/0.889	60.5	4.96	640
3	0.024/0.610	30.2	2.82	354
4	0.017/0.432	15.2	1.44	184
5	0.015/0.381	9.6	1.09	117
6	0.013/0.330	9.0	0.74	109
7	0.011/0.280	6.0	0.55	73
8	0.008/0.203	3.2	0.23	40
9	0.006/0.152	1.5	0.10	18

[a]Here, lpm, liters per minute.

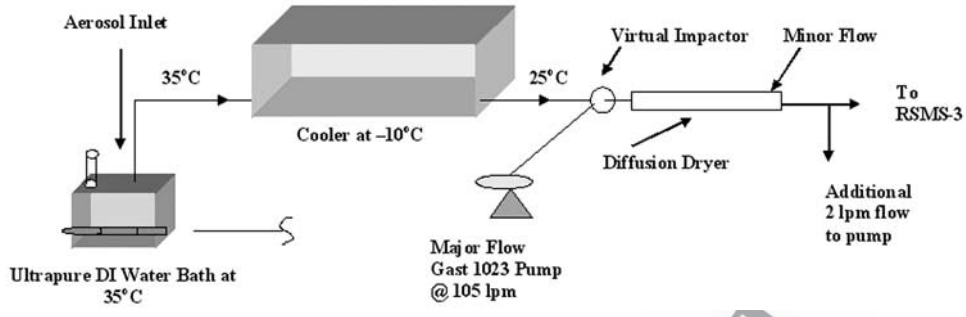

Figure 2. Schematic diagram of VACES fine plus ultrafine particle concentrator.

probe, a fraction of the total flow, referred to as the minor flow (typically 10–20% of the total flow), is allowed to pass through the probe, leaving particles larger than the cut point contained in a small fraction of the initial gases. The cut point of the virtual impactor used in VACES was 2.5 μm.

[9] In this experiment, the minor flow of the VACES concentrator was coupled to the RSMS-3 instrument; that is, the minor flow of the concentrator is directly connected to the sample port of the RSMS-3 mass spectrometer. The two instruments were operated at their original configurations, as described in the previous paragraphs in this section, without any modifications.

2.2. Data Analysis

[10] After firing each laser pulse, 5000 data points of the digitizer signals were acquired and examined by a computer. A single-particle mass spectrum was recorded when the height of any peak in the selected spectral region was greater than the predefined threshold value. Afterward, the data were transmitted from Pittsburgh Supersite to the UC Davis campus for storage and postprocessing. The single-particle mass spectra were first mass calibrated (converted from time to mass coordinates) covering the spectral range from m/z = −256 to m/z = +256. Spectra with a broad peak centering at m/z = 149 were caused by instrument emission and therefore were considered as background. After quality control to remove the background spectra, the calibrated spectra were integrated and normalized at integer m/z values and finally classified using the Adaptive Resonance Theory–2a (Art-2a) algorithm, which was first introduced by *Hopke and Song* [1997] for mass spectra analysis.

[11] The Art-2a algorithm uses the vector dot product as its similarity metric to classify the particles and is controlled by two parameters. The vigilance factor sets the similarity condition and the learning rate determines the rate at which the parameters adjust. The algorithm first selects each normalized spectrum in a random order and compares it to an existing set of weight vectors. If a winning weight vector is found to have the largest degree of similarity with the selected spectrum and its dot product with the corresponding particle vector is greater than the predefined vigilance factor, the selected spectrum is considered to belong to the class that the winning weight vector represents and then it is incorporated into the winning weight vector. In this case, the weight vector components are shifted toward the added spectrum's by the learning rate. If no weight vector satisfies the vigilance criterion with the selected spectrum, the particle vector becomes a new weight vector and is then added to the set of existing weight vectors. The first selected spectrum must be a new weight vector because there are no existing weight vectors to compare at that time. Once all spectra were selected, the whole procedure was repeated with a set of weight vectors produced in the previous iteration. *Phares et al.* [2001] validated the application of Art-2a algorithm in the analysis of single-particle spectra generated in laboratory with aerosols composing of single and mixed know chemical components. It was shown that a higher vigilance factor tended to overclassify (more classes than the real number) while a lower vigilance factor tended underclassify (less classes than the real) these laboratory-generated mass spectra. A vigilance factor of 0.6 was recommended to produce a class number that was very close to the real number [*Phares et al.*, 2001]; on this basis, the vigilance factor was predefined as 0.6 in this study. The final weight vectors are presented with equal-weighted averages of all spectra belonging to that class, in order to calculate the standard deviations in the peak heights for each class. Therefore no learning rate was used in this data analysis.

[12] Although RSMS-3 is a bipolar mass spectrometer measuring both positive and negative ions simultaneously, only positive spectra were analyzed with Art-2a algorithm and presented in this study. Previous research shows that most of negative spectra were contributed by sulfate, which is very difficult to ablate and detect in the fine and ultrafine particles sampled here [*Kane and Johnston*, 2001; *Lake et al.*, 2004]. Because of the large uncertainty in the detection of negative ion spectra, they were excluded in this study.

[13] The RSMS-3 hit rates were defined as the nonbackground particle hits divided by the corresponding measurement interval. Enhancements of the hit rate by VACESS concentrator were determined by ratios of the hit rate of concentrated air to that of ambient air. Ideal enrichments of particle concentration by VACES were predicted by the ratio of impactor's total-to-minor flow rate. The detection efficiency of RSMS-3 relative to the real aerosol concentration in the atmosphere will not be discussed in this work. Previously studies showed that the efficiency of RSMS instrument was about 10^{-6} and varied with particle size, shape, and chemical composition [*Kane and Johnston*, 2000; *Phares et al.*, 2002].

3. Results and Discussion

[14] Experiments were performed during two sampling periods in spring of 2002. The first, 5 March, provided

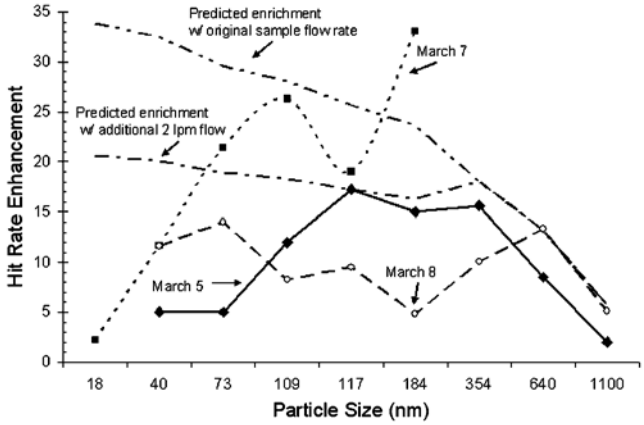

Figure 3. Enhancement of RSMS-3 hit rate by VACES particle concentrator. Predicted particle concentration enrichments were calculated using the ratio of VACES total-to-minor flow rate, where the 3 lpm flow rate passing through the RSMS-3 Nafion dryer was taken into account.

preliminary data and understanding of the use of the instruments together. The second, 7–8 March, was a more thorough test of the coupled system.

3.1. Data of 5 March 2002

[15] RSMS-3 was scheduled to measure one sample of unconcentrated ambient air followed by a concentrated sample at each particle size. The measurement time for each orifice (each particle size bin) was terminated by a maximum of 30 particle hits or 5 minutes whichever came first. Each measurement was repeated 2–3 times. The VACES concentrator was operated with a fixed major flow of 105 lpm. In total, 342 mass spectra from ambient air sample and 462 from sample with concentrator were recorded on 5 March 2002 after removal of the background spectra.

[16] Figure 3 shows the enhancement of RSMS-3 hit rates by VACES concentrator at different particle sizes observed in this study. Enrichments of particle concentration by VACES were also predicted on the basis of the ratios of total-to-minor flow rates of the impactor. Since the minor flow of the VACES concentrator was directly coupled to the RSMS-3 sample port, the minor flow of VACES was equal to the RSMS-3 sample flow listed in Table 1 plus the 3 lpm flow of the Nafion dryer which is not listed in Table 1. Diamonds connected with a solid line represent the 5 March results. The hit rate enhancement of RSMS-3 varies with particle size for a number of reasons. Since the VACES minor flow rate changed when RSMS-3 was sampling different particle sizes (see Table 1), while its major flow rate was fixed, the ratio of total-to-minor flow rate, and therefore the VACES concentration enrichment, changed with particle sizes, which is consistent with the predicted enrichment of particle concentration by VACES at large particle sizes and can readily be seen in Figure 3. With the VACES concentrator, particle hit rates of the RSMS-3 were increased by 10–17 times for the particles with sizes ranging from 109 to 354 nm. From size 640 nm to 1100 nm, the hit rate enhancements became smaller as the RSMS-3 sampling flow rate, and therefore the minor flow rate of the concentrator, increased. For the particles of 1100 nm, the enhancement of hit rates was only 2. The predicted enrichment was 5 at this point. Table 1 indicates that the flow rate at this particle size was greater than 15 lpm, which plus the 3 lpm of dryer flow was too high for the VACES concentrator to operate in its optimum range [*Sioutas et al.*, 1999].

[17] At the small particle side, the hit rate enhancements also decreased as the flow rate decreased which is contrary to the predicted particle concentration enrichment that increased. At these small particle sizes, the flow rates (about 3 lpm) into RSMS-3 were lower than the design conditions for the concentrator, so particle losses to the walls of the diffusion dryer would be substantial. On the other hand, the enrichment of particle concentration by VACES is affected to a large extent by the actual minor flow ratio and deviates from its ideal value as this ratio becomes smaller (i.e., less than about 5%). This is because as this minor flow decreases, particle losses mostly on the collection nozzle of the virtual impactor increase, thereby decreasing the overall enrichment [*Marple and Chien*, 1980; *Sioutas et al.*, 1994]. This is the case also with the virtual impactors used in the VACES to concentrate the grown ultrafine particles [*Sioutas et al.*, 1999]. Despite these losses, the hit rate enhancements at 40 and 73 nm were about 5. Accuracy of the real flow rate measurement is another factor in difference between the predicted VACES concentration enrichment and RSMS-3 hit rate enhancement. The ablation ability of RSMS-3 for different particle sizes [*Kane and Johnston*, 2000] would be another cause for the difference. It should be emphasized that this experiment was conducted with the RSMS-3 and VACES in their original configurations and the main premise of this research was to find out problems in coupling the two instruments together and ways to fix them, but no efforts were made to achieve the maximum enhancement of RSMS-3 hit rates.

[18] All single-particle mass spectra obtained on 5, 7, and 8 March were divided into two groups, with and without the concentrator, to calculate the hit rate enhancements and

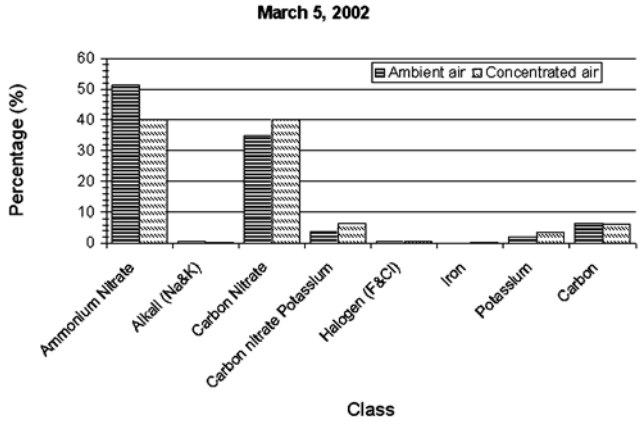

Figure 4. Comparison of chemical classes between ambient air and concentrated air measured on 5 March 2002.

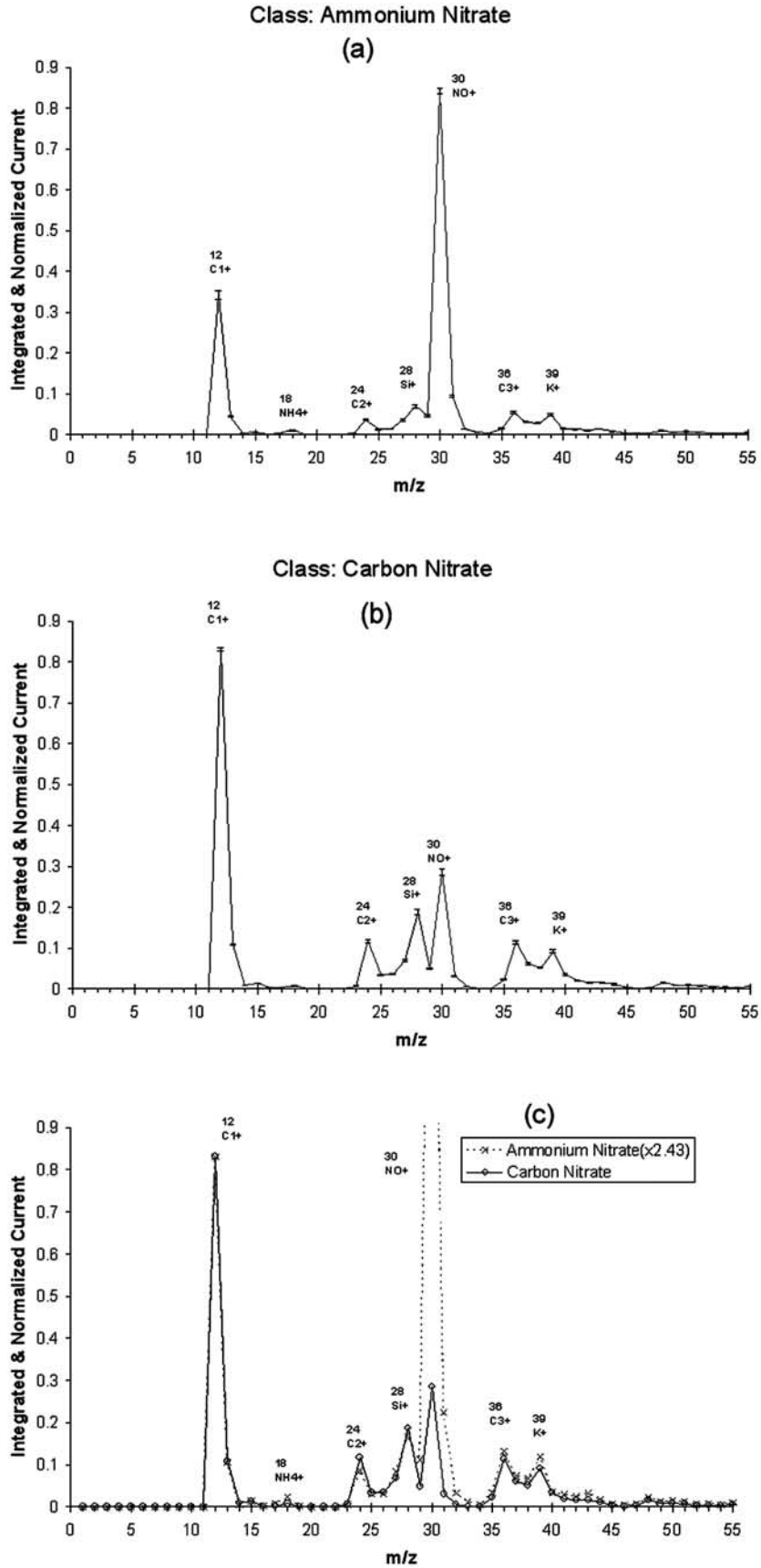

Figure 5. Average spectra of (a) ammonium nitrate and (b) carbon nitrate and (c) comparison between the two average spectra. The ammonium nitrate spectrum has been scaled up by 2.43 in Figure 5c to show the similarity between the two spectra.

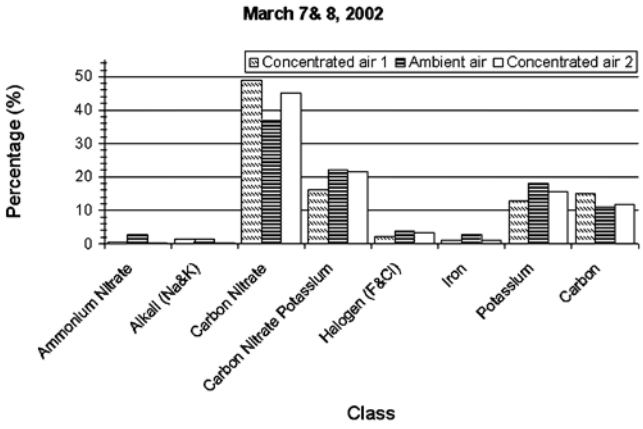

Figure 6. Same as Figure 4 but for 7–8 March 2002. The concentrated air was sampled immediately before (concentrated air 1) and after (concentrated air 2) the ambient air.

classified using Art-2a algorithm. All spectra were partitioned into 8 composition classes. Each of the eight classes represented more than 10 particles and those classes containing less 10 particles were considered minor and not presented. Figure 4 shows the fractions of total hits for each class observed on 5 March. The two major classes were ammonium nitrate (nitrate peak is domain in the spectra) and carbon nitrate (carbon peaks are domain in the spectra with a small nitrate peak), whose average spectra are shown in Figures 5a and 5b. Without the concentrator, about 51% of the particles were in the ammonium nitrate class and about 35% particles were in the carbon nitrate class, while their values were about 40% and 40%, respectively, when the concentrator was used. Figure 5c compares the average spectrum of the ammonium nitrate class with the one in the carbon nitrate class. The two spectra are very similar except for the NO^+ peak at m/z = 30 where the peak in the carbon nitrate class was much lower than in the ammonium nitrate class. Thus it appears that the concentrator might introduce a compositional change in a fraction of the particles, primarily shifting nitrate from particles in the ammonium nitrate class to those in the carbon nitrate class. This shift could be also due to a change in atmospheric composition during the experiment, so experiments on 7 and 8 March were designed to address this potential ambiguity. Including the effects of changes in chemical position of ambient air, the statistical uncertainty in RSMS-3 measurements, and the coupling with particle concentrator, in total about 8% particles were shifted from the ammonium nitrate class to the carbon nitrate class during the experiments on 5 March. More discussion regarding to this shift will be made in the following sections.

3.2. Data of 7 and 8 March 2002

[19] The RSMS-3 operating schedule was adjusted to measure one sample with concentrated air, one without, and again one with, at each particle size to separate changes in particle composition due to ambient conditions from those due to the concentrator. In order to obtain a more statistically significant sample, the measurement time was terminated at 30 particle hits at each particle size without setting a time limit. On 8 March, an additional 2 lpm was drawn from the minor flow port through diffusion dryer of the concentrator when RSMS-3 was sampling particles at sizes from 40 to 184 nm, in order to keep the changes in the ratio of total-to-minor flow rates small and minimize small particle losses. In total, 227 particles were collected without the concentrator and 701 with after removal of the background spectra.

[20] The hit rate enhancements are shown in Figure 3 for 7 March (closed squares) and 8 March (open circles). Decrease of the hit rate enhancement for small particles can still be seen on 7 March, but this dependence on RSMS-3 flow rate was partially corrected by pulling out the additional 2 lpm. On 7 March the hit rate enhancement of RSMS-3 at 184 nm was even higher than the predicted VACES enrichment of particle concentration, which is likely not true and might be caused by the removal of the background spectra. The causes for day-to-day hit rate variation, evident in Figure 3, may be due to variation in ambient conditions, RSMS-3 operating conditions such as laser intensity and laser beam alignment, or imprecise removal of background spectra.

[21] Class comparisons between samples collected with and without the concentrator on 7 and 8 March are shown in Figure 6. The four major classes were carbon nitrate (as shown in Figure 5b), carbon nitrate potassium, potassium, and carbon. Particles in the ammonium nitrate class were not observed on these days. The experiments of 7 and 8 March were designed to sample concentrated particles immediately before and after ambient particles to identify whether or not a shift in particle composition occurred during the sampling period. There is a 4% difference in the particle fractions between the two concentrated samples that could be due to either change in ambient air or instrument drift. A 10% difference is also seen in the carbon nitrate class between the ambient air and the average of the two concentrated samples indicating a possible class shift from other nitrate containing classes to carbon nitrate.

3.3. Causes of the Class Shift

[22] Figures 4 and 6 indicate that about 8–10% particles shifted from the ammonium nitrate class (or other nitrate containing classes) to the carbon nitrate class during the experiments on 5, 7, and 8 March when the RSMS-3 was coupled with the VACES particle concentrator. As discussed, changes in the ambient air, operational conditions of the RSMS-3, and artifacts caused by the VACES particle concentrator are the possible sources for the observed differences. This section will address more possible causes for the class shift.

[23] Figures 7a–7d compare the chemical classes between concentrated particles and ambient particles at different particle sizes measured on 5, 7, and 8 March 2002. Although the RSMS-3 can measure nine sizes of particles as given in Table 1, only two size ranges, a small size (40–117 nm) representing ultrafine particles and a large size (184–1100 nm) for the fine particles minus ultrafines, are grouped and shown in these figures in order to present statistically significant results. On 5 March the class shift from ammonium nitrate to carbon nitrate of ultrafine particles (Figure 7a) is the same pattern as the average of all sizes (Figure 4) but the shift of fine particles (Figure 7b) is

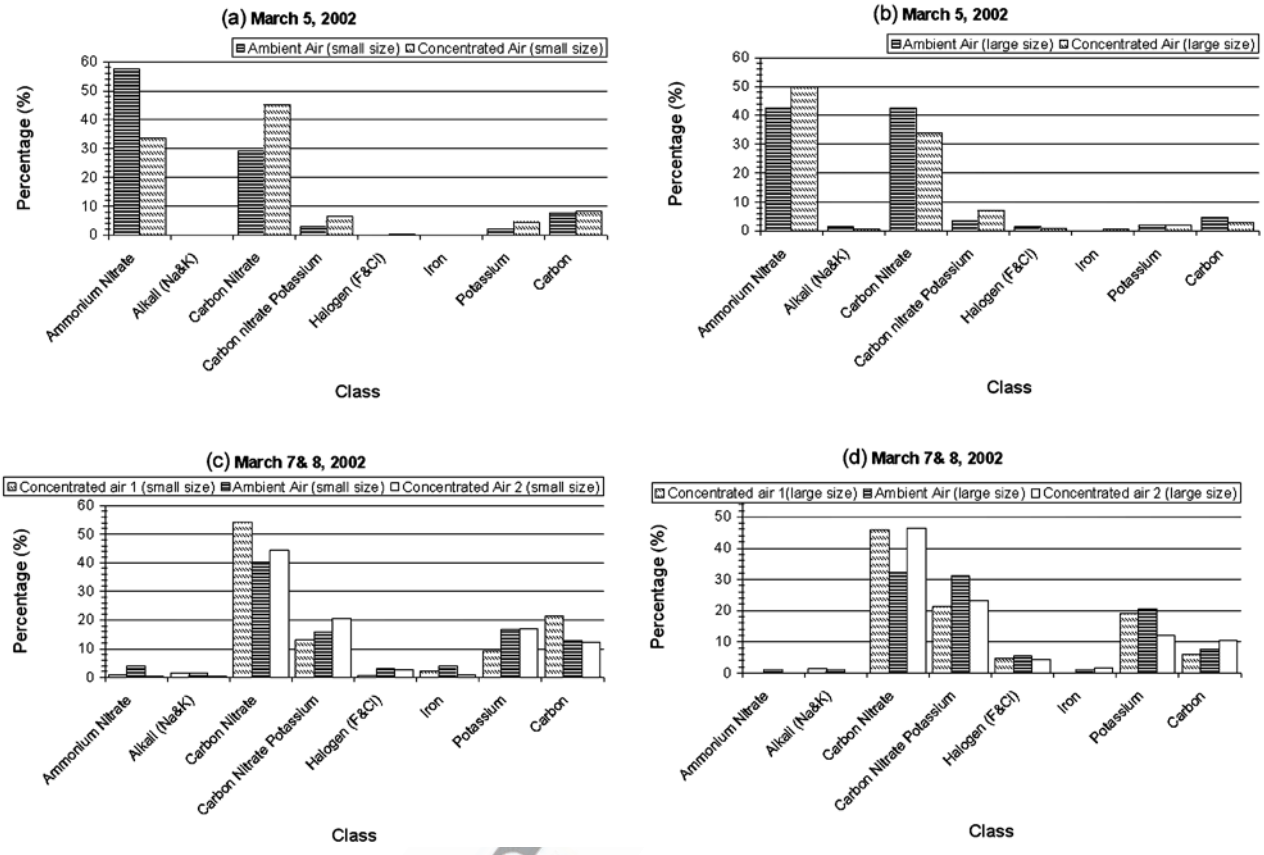

Figure 7. Same as Figure 4 but (a) for small size (ultrafine) particles of 5 March 2002 between 40 and 117 nm, (b) for large size (fine) particles of 5 March 2002 between 184 and 1100 nm, (c) for small size (ultrafine) particles of 7–8 March between 40 and 117 nm, and (d) for large size (fine) particles of 7–8 March between 184 and 1100 nm.

opposite. By comparison, on 7 and 8 March, the shifts at both fine and ultrafine particles (Figures 7c and 7d) are the same direction as that of the average. Observation by RSMS-3 on these days did not indicate any dependence of the class shift on particle sizes because the shift directions were random. From this point of view, it is thus unlikely that the VACES particle concentrator introduced the shift of particles from one class to another. If the concentrator did introduce such a shift, the patterns of the class shift should not change day-by-day.

[24] Figure 5c shows that the average spectra for the ammonium nitrate and carbon nitrate classes are identical when scaled to the C_1^+ peak heights, except for the height of the NO^+ peaks. Therefore it appears that the two classes have similar underlying carbonaceous cores with varying amounts of ammonium nitrate condensed, presumably due to varying particle age. Figure 8 shows the frequency distribution of particles from both classes as a function of the logarithm of the NO^+/C_1^+ peak ratio. Areas under each curve in Figure 8 are normalized to 1. It is seen that the frequency of ammonium nitrate class has a maximum at $NO^+/C_1^+ > 1$, while the maximum of carbon nitrate class is located at $NO^+/C_1^+ < 1$. There is a valley between the two maxima near $NO^+/C_1^+ = 1$. The Art-2a algorithm breaks the two classes near this valley. Since the valley is not very pronounced and in fact the distribution between the ammonium nitrate and carbon nitrate classes is more of a

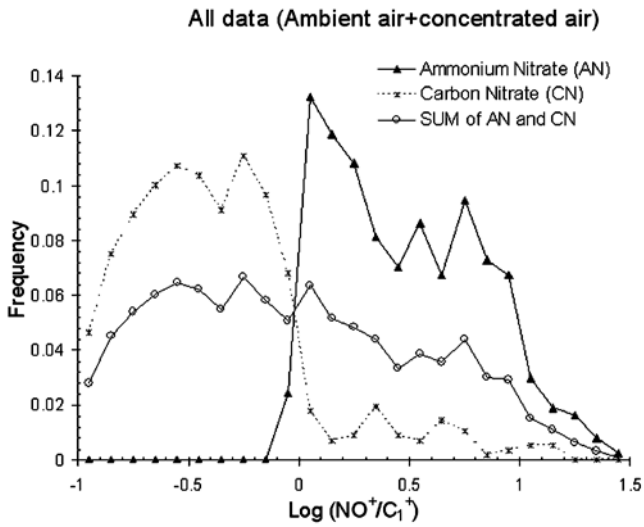

Figure 8. Frequency of the ratios of NO^+ peak to C_1^+ peak of ammonium nitrate class, carbon nitrate class, and sum of the two classes. Areas under each curve are normalized to 1.

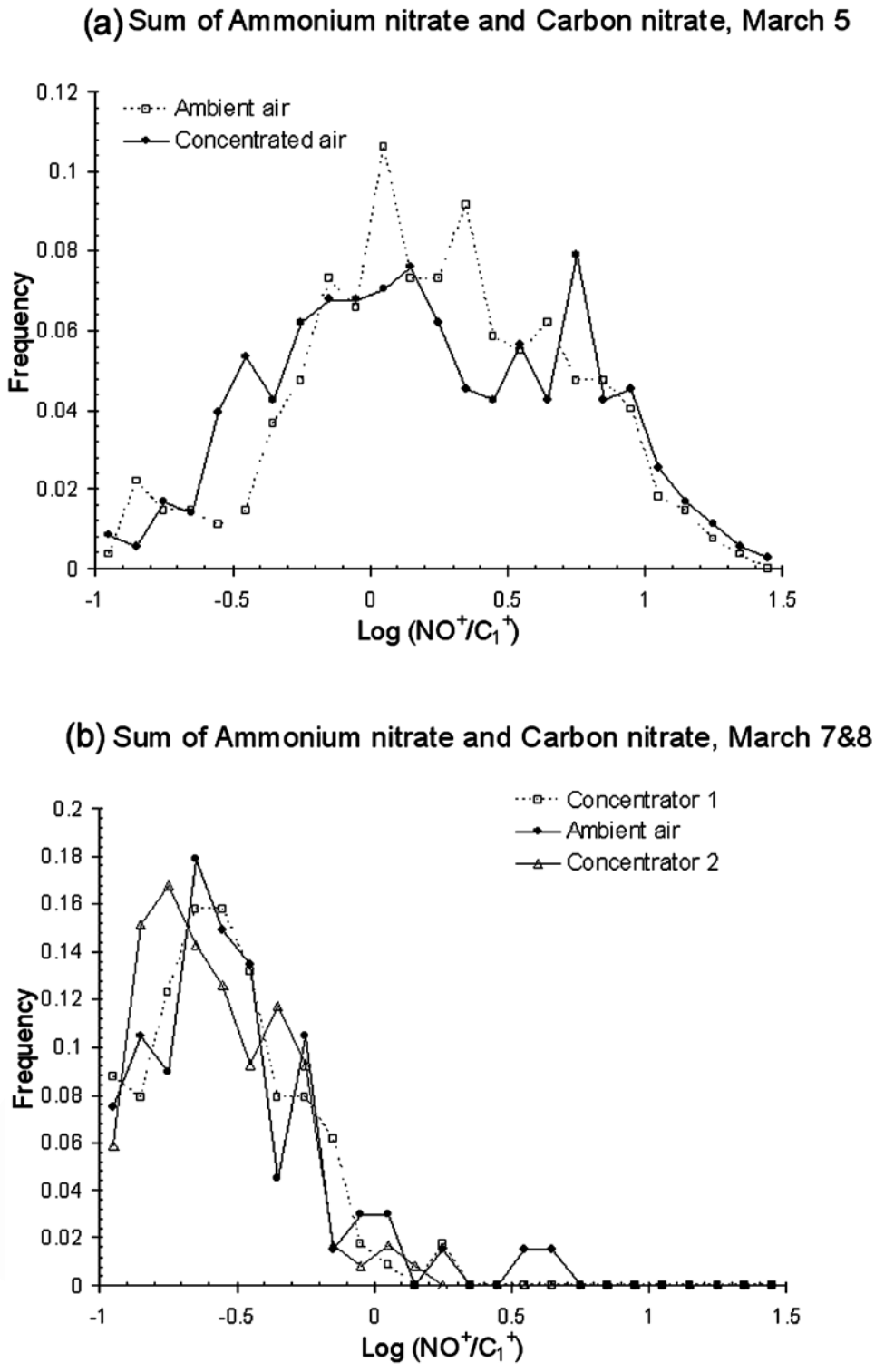

Figure 9. Comparisons of the frequency between ambient air and concentrated air measured on (a) 5 March 2002 and (b) 7–8 March 2002. Each curve is the sum of the ammonium nitrate class and the carbon nitrate class. Areas under each curve are normalized to 1.

continuous distribution, subtle differences between ammonium nitrate class and carbon nitrate class near $NO^+/C_1^+ = 1$ can move particle spectra from one class to the other. The atmospheric conditions, instrument operating conditions, and the Art-2a initial conditions could cause this movement. It can also be seen in Figure 8 that some of the high NO^+/C_1^+ particles were classified as carbon nitrate, which may be due to other peak information, since when the Art-2a algorithm

compares a selected spectrum with the existing set of weight vector, all peaks in the spectrum make contribution to the vector dot product. Therefore, when the contribution of other peaks to the dot product becomes more significant, the Art-2a may shift the class from one to another.

[25] Comparisons of these frequency distributions for ambient air and concentrated air are shown in Figures 9a and 9b for 5 March and 7 and 8 March, respectively. On 7 and 8 March the frequency distribution was skewed toward the $NO^+/C_1^+ < 1$ (see Figure 9b) indicating that on that day carbon nitrate particles (carbonaceous particles with a small amount of nitrate condensed on them) were observed much more frequently than ammonium nitrate particles (carbonaceous particles with a lot of nitrate condensed on them). Figure 6 shows the same results. Since both ammonium nitrate and carbon nitrate particle classes were observed in more equal proportions on 5 March (see Figure 4), the frequency distribution appears on both sides of $NO^+/C_1^+ = 1$ as shown in Figure 9a. There appear to be no significant difference in the frequency distributions between ambient and concentrated samples on both days and that the class shift from ammonium to carbon nitrate was not due to the particle concentrator.

4. Summary and Conclusions

[26] Our field evaluation of coupling VACES and RSMS-3 resulted in the following conclusions:

[27] 1. By coupling with the VACES concentrator, hit rates of the RSMS-3 single-particle mass spectrometer increased by 5–20 times except when RSMS-3 sampled the smallest and largest particle sizes where its flow rate was off the optimum configuration of the VACES concentrator.

[28] 2. Small differences in chemical composition were observed between samples with and without the VACES particle concentrator. The shift of 8–10% particles from one class to another could be caused by the changes in the composition of ambient air, or due to statistical variation in RSMS-3 measurements, or spectrum classification. There was no evidence showing that the VACES particle concentrator introduced the particle shift.

[29] 3. The minor flow rates of the VACES concentrator must be in its optimum range to effectively couple it to RSMS-3. Outside this range, the minor flow is either too high, resulting in a low concentration enhancement, or too low, causing ultrafine particle loss. Therefore it is necessary to control the minor flow rate of VACES in the coupling system when RSMS-3 samples different sizes of particles.

[30] 4. Since Art-2a judges class membership on the basis of a single vigilance factor, it broke a carbonaceous particle distribution with a wide range of ammonium nitrate content into two composition classes. Better algorithms should be developed that can identify distributions of composition within a class.

[31] **Acknowledgments.** This work was supported by EPA and DOE funding for the Pittsburgh Supersite (Y.Z., K.J.B., and A.S.W.) and the Southern California Particle Center and Supersite (SCPCS) funded by the U.S. EPA (STAR award R82735201) (C.M., P.M.F., and C.S.). This manuscript has not been subjected to the EPA peer and policy review and therefore does not necessarily reflect the views of the Agencies. No official endorsement should be inferred.

References

Bein, K. J., Y. Zhao, A. S. Wexler, and M. V. Johnston (2005), Speciation of size-resolved individual ultrafine particles in Pittsburgh, Pennsylvania, *J. Geophys. Res.*, *110*, D07S05, doi:10.1029/2004JD004708, in press.

Donaldson, K., X. Y. Li, and W. MacNee (1998), Ultrafine (nanometer) particle mediated lung injury, *J. Aerosol Sci.*, *29*, 553–560.

Finlayson-Pitts, B. J., and J. N. Pitts (1986), *Atmospheric Chemistry: Fundamentals and Experimental Techniques*, John Wiley, Hoboken, N. J.

Geller, M. D., S. Kim, C. Misra, C. Sioutas, B. A. Olson, and V. A. Marple (2002), A methodology for measuring size-dependent chemical composition of ultrafine particles, *Aerosol Sci. Technol.*, *36*, 748–762.

Heyder, J., P. Brand, J. Heinrich, A. Peters, G. Scheuh, T. Tuch, and E. Wichmann (1996), Size distribution of ambient particles and its relevance to human health, paper presented at 2nd Colloquium on Particulate Air Pollution and Health, U.S. Environ. Prot. Agency, Park City, Utah, 1–3 May.

Hopke, P. K., and X. Song (1997), Classification of single particles by neural networks based on the computer-controlled scanning electron microscopy data, *Anal. Chim. Acta*, *348*, 375–388.

Kane, D. B., and M. V. Johnston (2000), Size and composition biases on the detection of individual ultrafine particles by aerosol mass spectrometry, *Environ. Sci. Technol.*, *34*, 4887–4893.

Kane, D. B., and M. V. Johnston (2001), Enhancing the detection of sulfate particles for laser ablation aerosol mass spectrometry, *Anal. Chem.*, *73*, 5356–5369.

Kim, S., M. C. Chang, D. Kim, and C. Siouats (2000), A new generation of portable coarse, fine, and ultrafine particle concentrators for use in inhalation toxicology, *Inhalation Toxicol.*, *12*, 121–137.

Kim, S., P. Jaques, M. C. Chang, J. R. Froines, and C. Sioutas (2001a), A versatile aerosol concentrator for simultaneous in vivo and in vitro evaluation of toxic effects of coarse, fine and ultrafine particles: Part I: Laboratory evaluation, *J. Aerosol Sci.*, *32*, 1281–1297.

Kim, S., P. Jaques, M. C. Chang, C. Xiong, S. K. Friedlander, and C. Sioutas (2001b), A versatile aerosol concentrator for simultaneous in vivo and in vitro evaluation of toxic effects of coarse, fine and ultrafine particles: Part II: Field evaluation, *J. Aerosol Sci.*, *32*, 1299–1314.

Koutrakis, P., J. M. Wolfson, J. L. Slater, M. Brauer, J. D. Spengler, R. K. Stevens, and C. L. Stone (1988), Evaluation of an annular denuder filter pack system to collect acidic aerosol and gases, *Environ. Sci. Technol.*, *22*, 1463–1468.

Lake, D. A., M. P. Tolocka, M. V. Johnston, and A. S. Wexler (2003), Mass spectrometry of individual particles between 50 and 750 nm in diameter at the Baltimore Supersite, *Environ. Sci. Technol.*, *37*, 3268–3274.

Lake, D. A., M. P. Tolocka, M. V. Johnston, and A. S. Wexler (2004), The character of single particle sulfate in Baltimore, *Atmos. Environ.*, *38*, 5311–5320.

Li, N., C. Sioutas, A. Cho, D. Schmitz, C. Misra, M. Wang, T. Oberley, J. R. Froines, and A. Nel (2003), Ultrafine particulate pollutants induce oxidative stress and mitochondrial damage, *Environ. Health Perspect.*, *111*, 455–460.

Marple, V. A., and C. M. Chien (1980), Virtual impactors: A theoretical study, *Environ. Sci. Technol.*, *14*, 976–985.

Middha, P., and A. S. Wexler (2003), Particle focusing characteristics of sonic jets, *Aerosol Sci. Technol.*, *37*, 907–915.

Peters, A., D. W. Dockery, J. Heinrich, and H. E. Wichmann (1997), Short-term effects of particulate air pollution on respiratory morbidity in asthmatic children, *Eur. Respir. J.*, *10*, 872–879.

Phares, D. J., K. P. Rhoads, A. S. Wexler, D. B. Kane, and M. V. Johnston (2001), Application of the Art-2a algorithm to laser ablation aerosol mass spectrometry of particle standards, *Anal. Chem.*, *73*, 2338–2344.

Phares, D. J., K. P. Rhoads, and A. S. Wexler (2002), Performance of a single ultrafine particle mass spectrometer, *Aerosol Sci. Technol.*, *36*, 583–592.

Phares, D. J., K. P. Rhoads, M. V. Johnston, and A. S. Wexler (2003), Size-resolved ultrafine particle composition analysis: 2. Houston, *J. Geophys. Res.*, *108*(D7), 8420, doi:10.1029/2001JD001212.

Rhoads, K. P., D. J. Phares, A. S. Wexler, and M. V. Johnston (2003), Size-resolved ultrafine particle composition analysis: 1. Atlanta, *J. Geophys. Res.*, *108*(D7), 8418, doi:10.1029/2001JD001211.

Sioutas, C., P. Koutrakis, and B. A. Olson (1994), Development of a low cutpoint virtual impactor, *Aerosol Sci. Technol.*, *21*, 223–235.

Sioutas, C., S. Kim, and M. C. Chang (1999), Development and evaluation of a prototype ultrafine particle concentrator, *J. Aerosol Sci.*, *30*, 1001–1017.

Tolocka, M. P., D. A. Lake, M. V. Johnston, and A. S. Wexler (2004a), Number concentrations of fine and ultrafine particles containing metals, *Atmos. Environ.*, *38*, 3263–3273.

Tolocka, M. P., D. A. Lake, M. V. Johnston, and A. S. Wexler (2004b), Ultrafine nitrate particle events in Baltimore observed by real-time single particle mass spectrometry, *Atmos. Environ.*, *38*, 3215–3223.

Tolocka, M. P., D. A. Lake, M. V. Johnston, and A. S. Wexler (2005), Size-resolved fine and ultrafine particle composition in Baltimore, Maryland, *J. Geophys. Res.*, *110*, D07S04, doi:10.1029/2004JD004573, in press.

Willeke, K., and P. A. Baron (1993), *Aerosol Measurement: Principles, Techniques, and Applications*, Van Nostrand Reinhold, Hoboken, N. J.

K. J. Bein, Department of Land, Air and Water Resources, University of California, Davis, One Shields Avenue, Davis, CA 95616, USA. (kjbein@ucdavis.edu)

P. M. Fine, C. Misra, and C. Sioutas, Department of Civil and Environmental Engineering, University of Southern California, 3620 S. Vermont Avenue, Los Angeles, CA 90089, USA.

A. S. Wexler and Y. Zhao, Department of Mechanical and Aeronautical Engineering, University of California, Davis, One Shields Avenue, Davis, CA 95616, USA. (aswexler@ucdavis.edu; yjzhao@ucdavis.edu)